ACS Catalysis

Review

pubs.acs.org/acscatalysis

Heterogeneous Catalysts for the Guerbet Coupling of Alcohols

Joseph T. Kozlowski and Robert J. Davis*

Department of Chemical Engineering, University of Virginia, 102 Engineers Way, Charlottesville, Virginia 22904-4741, United States

ABSTRACT: Alcohol coupling, also known as the Guerbet reaction, is a potentially important process to increase the value of short chain alcohols. Metal oxides, metal phosphates, and supported transition metals, such as copper, are important components of heterogeneous catalysts for the reaction. However, the wide variety of catalyst compositions, reaction conditions, and reactor configurations used to study the reaction complicate a direct comparison of various catalysts. In this review, rates over different catalysts will be compared, the influences of the acid and base properties of the catalyst on product selectivity will be presented, and possible reaction paths to accomplish alcohol coupling will be discussed.

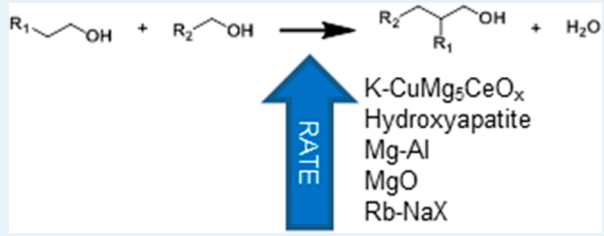

KEYWORDS: *Guerbet reaction, alcohol condensation, alcohol dehydrogenation, oxide catalysts, alcohol coupling*

1. INTRODUCTION

The Guerbet reaction involving the coupling of two alcohol molecules is named after Marcel Guerbet, who studied the self-coupling of butan-1-ol to produce the branched saturated alcohol, 2-ethylhexan-1-ol, in the 1890s.[1] Depending on the types of alcohols used in the reaction (primary versus secondary, long chain versus short chain), branched or unbranched products will be formed. In addition, when different alcohols are present in the reaction, both self-coupling and cross-coupling reactions can occur. Typically, reference to "Guerbet alcohols" is often to highly branched, saturated alcohols prepared by the condensation of two primary alcohols, and these products are important in the production of surfactants. Much of the work on Guerbet reactions over heterogeneous catalysts, however, focuses on the conversion of short-chain alcohols, less than about C_4. Since surfactant production usually involves at least part of the catalyst in the fluid phase, most of that literature is beyond the scope of this review. For a more thorough discussion of the production of Guerbet alcohol-derived surfactants, please see the review on the topic by O'Lenick.[2] Although some generalizations regarding the mechanism of alcohol coupling can be obtained from studies involving homogeneous catalysts, this review emphasizes the work on heterogeneous catalysts for the reaction.

Early patents describe mixtures of metal oxides as catalysts for the reaction. In 1931, ethanol coupling in the presence of H_2 was observed over mixtures of MgO, Al_2O_3, and CuO_x between 473 and 573 K.[3] Self-condensation of ethanol at high pressures (6.1 to 14.2 MPa) and temperatures ranging from 473 to 673 K was also patented over materials containing copper and magnesium oxide in 1933.[4] Coupling of larger alcohols (C_{4+}) with H_2 over mixtures of MgO, Al_2O_3, and CuO_x received a patent in 1937.[5] The coupling of various alcohols over soda lime (calcium hydroxide and alkali hydroxides) between 648 and 853 K was patented in 1953.[6] Between 1956 and 1970, several patents described how alkali metal salts dissolved in alcohol with the addition of an insoluble dehydrogenation agent such as copper or nickel were effective at coupling various alcohols (C_2–C_{10+}).[7−10] Subsequent work with methanol and ethanol demonstrated effective coupling reactions catalyzed by γ-Al_2O_3 together with an alkali metal salt and platinum group metal between 473 and 673 K and 6.9–13.9 MPa.[11] Soon thereafter, soluble alkali metal or alkali metal salt combined with an insoluble lead salt were reported as alcohol coupling agents in a patent in 1977.[12] By the mid-1980s, alkali metals were well recognized as important components of alcohol coupling catalysts.[13,14] Indeed, many patents in the field recognize the importance of combining an alkali metal compound with a separate component capable of catalyzing hydrogenation and dehydrogenation, such as Cu and Ni.[15−23]

A clear picture emerges from the patent literature that two features of the catalyst are required for the alcohol coupling reaction. The first feature is related to the acidity and basicity of the catalyst. Alcohol coupling systems commonly have basic materials in the form of alkali metal, hydroxide, or salt dissolved in the reaction medium or, in the case of heterogeneous catalysts, have a solid base, such as magnesia, as a critical component. The second feature of a catalyst needed for alcohol coupling is the ability to facilitate dehydrogenation of the alcohol at the reaction temperature. Some typical metals used as dehydrogenating agents include platinum,[11] nickel,[13,24,25] and copper.[26−29] Some nonmetals, such as the solid base MgO, can catalyze dehydrogenation of alcohols at sufficiently high temperatures.

Many recent publications on Guerbet reactions over heterogeneous catalysts involve the upgrading of short-chain alcohols into longer-chain, saturated alcohols, such as the self-

Received: November 28, 2012
Published: May 21, 2013

   dx.doi.org/10.1021/cs400292f | ACS Catal. 2013, 3, 1588–1600

coupling of ethanol to produce butan-1-ol. This is an attractive process since the properties of butan-1-ol alleviate some of the problems with ethanol as a fuel or fuel additive. Butan-1-ol has an energy density closer to gasoline than ethanol and does not have the same propensity as ethanol to absorb water. Unlike ethanol, however, butan-1-ol is produced mainly from fossil resources.[30] Butan-1-ol has many current commercial uses, such as a perfume additive, flavoring agent, solvent, and chemical intermediate.[30] Upgrading of other short-chain alcohols is also possible, with the caveat that methanol cannot self-couple through the Guerbet reaction. Methanol can be coupled with alcohols having 2 or more carbon atoms.

The Guerbet reaction involves a complex sequence of many other reactions (dehydrogenation, aldolization, dehydration, and hydrogenation) that could be the legitimate subjects of individual reviews. Nevertheless, the overall reaction path needs to be discussed in light of the various catalysts used for the reaction. Although this review is by no means an exhaustive analysis on the topic, hopefully, it will provide an introduction to the challenges of Guerbet coupling reactions over heterogeneous catalysts that are in need of more attention.

2. REACTION PATH

Alcohol coupling has been proposed to progress by two different routes. The most commonly accepted path involves an aldolization reaction as the C−C bond forming step with a nonadsorbed carbonyl-containing intermediate. This route includes four different types of reactions: dehydrogenation, aldolization, dehydration, and hydrogenation. This sequence is supported by several pieces of information provided below:

- The intermediates of ethanol self-coupling to produce butan-1-ol included ethanal, but-2-en-1-al, and other characteristic aldolization intermediates.[29,31−33]
- Aldol intermediates, such as but-2-en-1-al, presumably formed during ethanol self-coupling, were hydrogenated in the presence of alcohol at reaction conditions.[32]
- Ethanal or but-2-en-1-al each produced butan-1-ol over MgO−CuO−MnO in the presence of H_2.[34]
- Reactions of ^{13}C-labeled ethanal and unlabeled ethanol produced mostly labeled coupling products over a mixed oxide (0.8 wt % K on Mg_5CeO_x) at low surface residence times.[29]
- Aldol condensation occurred readily at the temperatures used in Guerbet reactions.[29,32,35]
- The rate of production of the coupled product was proportional to aldehyde concentration.[29,33,36]

This generally accepted sequence of steps, which has been discussed in many publications, is summarized below.

The first step in the alcohol coupling reaction is the dehydrogenation of the reagent alcohol to produce an intermediate aldehyde or ketone. Since aldol condensation occurs between two carbonyl-containing molecules, both alcohols involved in the coupling reaction must be dehydrogenated. Schemes 1 and 2 show the dehydrogenation of two primary alcohols. One aspect of this step that remains unclear is the location and chemical state of the hydrogen evolved. In the case of catalysts that include a transition metal, such as copper,

Scheme 1

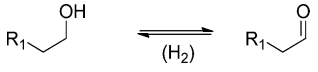

Scheme 2

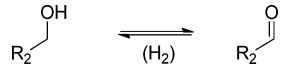

dihydrogen can be released from the surface after the dehydrogenation reaction, and the gas phase dihydrogen and aldehyde are in equilibrium with the alcohol. For mixed oxides, without transition metal cocatalysts, the location of the hydrogen is unclear: it may remain adsorbed on the surface to later hydrogenate products, it may desorb as dihydrogen, or the dehydrogenation may be coupled to a hydrogenation step by the Meerwin−Ponndorf−Verley (MPV) reaction. Gines and Iglesia[29] observed that a copper-containing mixed metal oxide ($K-CuMg_5CeO_x$) had much higher rates of deuterium incorporation (from gas phase D_2) into the reactant alcohol as well as in the coupled products than the analogous catalyst without copper ($K-Mg_5CeO_x$). Because of the ambiguity of the fate of the hydrogen atoms, the hydrogen in these schemes will be indicated as (H_2).

Scheme 3 depicts the aldol addition step. Aldol reactions occur readily over basic catalysts and likely proceed through a

Scheme 3

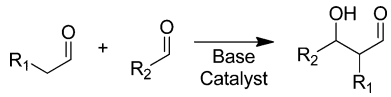

surface enolate.[37] The enolate acts as a nucleophile and attacks the other aldehyde or ketone present in the system. This addition reaction creates a bond between the α-carbon of one molecule with the carbonyl carbon of another molecule and is likely responsible for the branched nature of many Guerbet alcohols. For example, if two ethanal molecules undergo an aldol condensation, followed by hydrogenation, then the linear alcohol butan-1-ol is formed because the reactive intermediates are a primary enolate and an aldehyde. If a secondary enolate is formed, or an enolate attacks a ketone, that is, in the self-condensation of propan-1-ol or the condensation of propan-1-ol with propan-2-ol, a branched alcohol is formed. If the initial reactants are not the same alcohol (excluding methanol), there are four product options: two different cross-coupling products formed from the different enolates, and two self-coupling products. Selectivity to these products will be affected by the relative rates of dehydrogenation and enolate formation.

Scheme 4 shows the dehydration of the aldol addition product, which presumably occurs quite readily since the aldol

Scheme 4

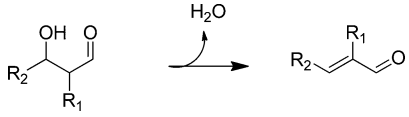

addition products are generally not observed. For many of the applications that involve liquid phase condensations with a soluble base, water is removed to prevent the formation of the undesirable carboxylic acid from the reactant or product aldehyde. Aldehyde oxidation to the acid product is known to occur when base, water, and a transition metal catalyst are present at 295 K,[38] which is a much lower temperature than that typically used in Guerbet reactions in the liquid phase

dx.doi.org/10.1021/cs400292f | ACS Catal. 2013, 3, 1588−1600

(>373 K). Not only is the carboxylic acid product undesirable in some cases but it also neutralizes the base catalyst. Removal of water to decrease the production of undesired acid is the subject of a patent in which distillation or a desiccant such as magnesia or calcium oxide was utilized.[17]

The final two steps in the sequence are represented in Schemes 5 and 6 as hydrogenation reactions, which might

Scheme 5

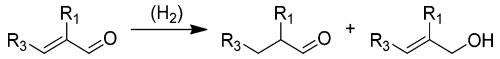

Scheme 6

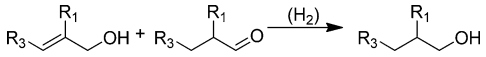

occur in either order. These steps can be accomplished on a hydrogenation catalyst, such as copper or nickel, if it is present on the catalyst or over a metal oxide at sufficiently high temperatures with an adequate hydrogen source, such as the reactant alcohol. The unsaturated intermediates have been observed by several groups.[29,31,32]

The interrelationships among these steps help explain why some catalysts are more effective than others. Over most basic solids, aldol condensation occurs rapidly and at much lower temperatures than those typically used in Guerbet reactions. For example, Guerbet reactions over MgO are typically performed near 673 K, whereas MgO can easily catalyze the aldol condensation of 2-propanone at room temperature or lower.[39−44] A high reaction temperature would suggest that a major hurdle during Guerbet coupling over MgO is the initial dehydrogenation of the alcohol to form the carbonyl intermediate, which explains why addition of a hydrogenation/dehydrogenation catalyst such as copper improves the performance of basic metal oxide catalysts.

A second possible reaction path for Guerbet coupling proposed by Yang and Meng[45] and Ndou et al.[46] involves a direct surface coupling reaction resulting in dehydration from the OH of one alcohol and the hydrogen attached to the α-carbon of a second. Although this proposed reaction (Scheme 7) involves two alcohols, the direct reaction of an aldehyde and

Scheme 7

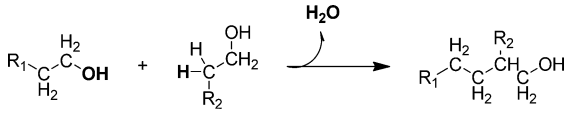

an alcohol is also considered (Scheme 8). This direct coupling mechanism was proposed after addition of reaction intermediates leading to, or produced from, an aldolization-type C−C bond forming step did not increase the rate of butan-1-ol production from ethanol. The analysis did not account for other factors that might affect the conversion of added reaction

Scheme 8

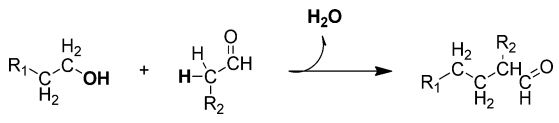

intermediates, such as a difference in the amount of surface hydrogen available for reaction or a high surface coverage of aldol intermediates formed from the alcohols. Although the direct coupling route has been proposed, there appears to be a general consensus in most of the literature that Guerbet coupling involves an aldol intermediate.

As discussed above, a gas phase carbonyl species is one likely candidate for the reaction intermediate in Guerbet coupling, but others suggest that the reaction does not necessarily require participation of a gas phase carbonyl. Evidence that some fraction of the final product is not produced from a gas phase carbonyl intermediate is derived from two observations. The first is a kinetic analysis of products observed as the space time of the reactants is changed. For ethanol conversion to butan-1-ol, ethanal and ethene appeared as primary products during the change in space time; however, a low but nonzero slope for butan-1-ol suggests that some of it may also form as a primary product of ethanol conversion.[31] In addition, Gines and Iglesia[29] added ^{13}C-labeled ethanal to a reaction of unlabeled ethanol over K−$CuMg_5CeO_x$ and K−Mg_5CeO_x and observed at low contact times that a minority of the C_4 product did not originate from the labeled ethanal.[29] Therefore, Guerbet coupling of ethanol over Mg/Al mixed oxides,[31] K−$CuMg_5CeO_x$,[29] and K−Mg_5CeO_x[29] was proposed to proceed via two different aldehyde intermediates, one involving a gas phase aldehyde and another that is completely surface-bound (without participation of a gas phase aldehyde intermediate). Even for the direct surface route depicted in this mechanism, the C−C bond-forming step is still a classical aldolization reaction, but with an aldehyde that remains adsorbed on the catalyst after being formed in the initial alcohol dehydrogenation step. Nagarajan also performed similar kinetic analysis on the products from ethanol coupling but concluded butan-1-ol and but-2-enal were secondary products over a MgO−CuO−MnO catalyst.[33] All of these studies generally support the importance of aldol coupling reactions as intermediate steps in the Guerbet reaction, although the exact details are still subject to debate.

The aldol intermediate produced in the self-coupling of ethanol has many final products that may be derived from it. One example is the production of buta-1,3-diene from the coupling of two ethanol molecules. This reaction has been commercialized in several locations, including the U.S., China, India, Poland, and the former USSR.[30] Two different processes have been used to produce buta-1,3-diene from ethanol: although the Lebedev process is performed in a one step, the Ostromislensky process is a two-step sequence in which ethanol is partially converted to ethanal in the first step, which is followed by aldolization and deoxygenation in the second step.

The single-step Lebedev process for the production of buta-1,3-diene from ethanol proceeds via the same reactions as the two-step Ostromislensky process, but over a single, multifunctional catalyst. Many of the catalysts that have been used in the single step process contain varying amounts of MgO, SiO_2, and Al_2O_3, with MgO being the majority component.[47] Other materials that have been used to produce buta-1,3-diene from ethanol include tantalum oxide, hafnia, zirconia, or alumina on silica;[47] Ni on a magnesium silicate;[48] sepiolite;[49] aluminated sepiolite;[50] and magnesia and silica.[51,52] A recent study by Jones et al. of many different materials supported on silica showed a Zn/Zr oxide on silica to have high activity.[53] They concluded that the optimal catalyst needs some acidic sites, but very strong acid sites will increase the selectivity to undesired products,

dx.doi.org/10.1021/cs400292f | ACS Catal. 2013, 3, 1588−1600

Table 1. Rates for Propan-1-ol and Ethanol Dehydration, Dehydrogenation, and Self-Coupling over MgO

reactant	surface area (m^2 g^{-1})	temp (K)	conversion	aldehyde concn (μmol L^{-1})	dehydrogenation rate (nmol m^{-2} s^{-1})	dehydration rate (nmol m^{-2} s^{-1})	coupling rate others (nmol m^{-2} s^{-1})	coupling rate saturated alcohol (nmol m^{-2} s^{-1})	unreported product rate (nmol m^{-2} s^{-1})	ref
ethanol	125	573	0.51	0.031	0.078	0.011	NR	0.058	0.0	71
propan-1-ol	50	573	1.5	3.8	0.25	NR	NR	2.2	0.92	35
propan-1-ol	50	623	3.0	6.9	0.50	NR	NR	4.0	2.2	35
ethanol	166	625	10	28	0.62	1.3	0.50	1.1	0.0	55
ethanol	166	658	20	42	1.0	2.9	1.0	2.0	0.10	55
propan-1-ol	50	673	7.5	37	2.9	NR	NR	8.2	5.6	35
propan-1-ol	50	723	28	119	10	NR	1.6	31	12	35
propan-1-ol	50	773	44	82	7.4	NR	NR	38	52	35

Table 2. Coverages of Ethanol and Reactive Intermediates Leading to Butan-1-ol on MgO at 673 K Derived from Steady-State Isotopic Transient Analysis of the Ethanol Coupling Reaction[66]

total flow rate (cm^3 min^{-1})	$\tau_{ethanol}$ (s)	coverage of ethanol $N_{ethanol}$ (μmol m^{-2})	butanol formation rate (nmol m^{-2} s^{-1})	$\tau_{butanol}$ (s)	coverage of intermediates to butanol $N_{butanol}$ (μmol m^{-2})
25	32	5.1	8.1	60	0.49
50	13	4.7	5.2	36	0.19
75	7.8	4.6	3.1	32	0.10

such as ethene and butane.[53] A thorough review on the topic by Toussaint and Marsh is an excellent resource for more information.[47] Materials exposing acid sites together with base sites, such as Mg/Al mixed oxides or hydroxyapatite, have produced some buta-1,3-diene in the product mixture from ethanol coupling to butan-1-ol.[54,55]

The industrially relevant molecule 2-methylpropene has also been produced from ethanol through a similar proposed aldol intermediate.[56] In this reaction, ethanol is fed to the reactor along with water, which probably facilitates the C−C bond breaking of the aldol products.[56] One potential sequence involves the coupling of ethanol followed by C−C bond cleavage to produce 2-propanone, which can then couple and undergo another C−C cleavage to produce 2-methylpropene. Each of these individual steps, ethanol to 2-propanone[57−61] and 2-propanone to 2-methylpropene,[41,62] has been explored, but only recently has the concerted reaction been completed over a Zn/Zr oxide catalyst.[56] As described earlier, a catalyst with appropriately weak acid sites is necessary, being careful to avoid the dehydration of ethanol to the undesired product ethene.

Another example in which alcohol coupling likely plays a role is in higher alcohol synthesis (HAS) from synthesis gas over basic materials. Although reactions to form alcohols with 1 or 2 carbon atoms clearly proceed in a different fashion, it has also been theorized that some of the longer-chain alcohols present in the product stream of HAS reactors is due to the aldol-based coupling of two smaller alcohols.[63−65] Alcohol coupling is expected because the reaction conditions of HAS are similar to those of Guerbet coupling, and the typical catalysts have all of the functions necessary for coupling to occur.

3. BASIC METAL OXIDE AND METAL PHOSPHATE CATALYSTS

3.1. MgO. Many different basic oxide materials have been used as catalysts for the Guerbet reaction. In particular, MgO appears to be the standard basic oxide to which many others are compared. Representative results from ethanol and propan-1-ol conversion over MgO are presented in Table 1. The rates presented in the table were converted to a consistent units basis, and the various examples are placed in order of increasing reaction temperature. Two factors seem to impact the coupling rate to form saturated alcohol: Higher temperatures obviously increase the coupling rate, as well as the dehydrogenation and dehydration rates. The second factor affecting the coupling rate is the intermediate aldehyde concentration. As mentioned above, the Guerbet reaction catalyzed by basic oxides likely occurs by two routes, with the majority of the product being formed from a gas phase aldehyde intermediate. As shown in Table 1, the minimum temperature to realize appreciable yields over MgO was apparently 573 K. Table 1 also includes the rate of formation of unreported product. Since Ndou et al.[35] do not report dehydration rates, a major component of the rate of unreported products in that case is most likely the result of dehydration of the reactant alcohol.

Very recently, our group used isotopic transient analysis to explore the coupling of ethanol over MgO.[66] The technique involves an abrupt switch in the ^{13}C content of the ethanol feed after the steady-state reaction of unlabeled ethanol has been achieved and then monitoring the incorporation of the ^{13}C label into the product stream as a function of time via mass spectrometry. After accounting for readsorption of products, the intrinsic time to turn over the active sites on the catalyst and the coverage of reactive intermediates leading to products can be determined. Surface coverages and the time constants associated with adsorbed ethanol and intermediates leading to butanol production over MgO at 673 K are summarized in Table 2. Three different flow rates were used to vary the residence time and, therefore, the ethanol conversion in the differential flow reactor. A very high coverage of ethanol was measured on MgO, roughly 50% of the exposed MgO surface pairs, whereas the coverage of reactive intermediates actually leading to products was more than an order of magnitude lower than that of ethanol. Results from in situ DRIFTS indicated the surface was covered primarily by ethoxide and hydroxide

dx.doi.org/10.1021/cs400292f | ACS Catal. 2013, 3, 1588−1600

Table 3. Rates for Ethanol Dehydration, Dehydrogenation, and Self-Coupling over Al_2O_3 and Mg/Al Mixed Oxides

material	surface area (m^2 g^{-1})	temp (K)	conversion	aldehyde concn (μmol L^{-1})	dehydrogenation rate (nmol m^{-2} s^{-1})	dehydration rate (nmol m^{-2} s^{-1})	coupling rate saturated alcohol (nmol m^{-2} s^{-1})	ref
Mg/Al 8.1	114	573	4.4	47	1.3	0.017	0.27	71
Mg/Al 4.6	184	573	3.6	42	0.71	0.019	0.14	71
Mg/Al 3.2	238	573	5.0	23	0.31	0.022	0.28	71
Mg/Al 3	142	523	4.0	2.6	0.20	0	1.0	54
Mg/Al 3	142	573	9.0	11	0.91	0	1.4	54
Mg/Al 3	142	623	21	28	2.7	4.5	2.7	54
Mg/Al 3	142	673	50	110	11	17	3.6	54
Mg/Al 3	142	723	87	242	27	33	2.2	54
Mg/Al 3	142	773	98	340	40	37	1.0	54
Mg/Al 1.1	231	573	9.7	6.0	0.081	0.16	0.51	71
Mg/Al 0.5	298	573	13	6.9	0.072	0.17	0.14	71
Al_2O_3	388	573	86	2.8	0.022	7.9	0	71

produced in the dissociative adsorption of ethanol. The intrinsic time constant for the production of butan-1-ol from ethanol over MgO at 673 K was calculated by subtracting the average residence time of ethanol from that of butan-1-ol to remove the chromatographic adsorption and desorption of the product alcohol throughout the catalyst bed, which gave a value of 25 s.[66] The intrinsic turnover frequency of the reaction is simply the inverse of the time constant, which in this case was 0.04 s^{-1}. An important aspect of this method is that no separate measure of the active site density in the reactor is needed to estimate the turnover frequency. This TOF from isotopic transient analysis (0.04 s^{-1})[66] is lower than the TOF for acetone aldol condensation at 299 K over MgO (0.10 s^{-1}),[67] which supports the idea that the production of butan-1-ol is influenced by the large surface coverage of ethoxide on MgO during ethanol coupling. As observed in other studies, the rate of butan-1-ol formation was proportional to the ethanal concentration. Evidently, the surface of MgO was predominately covered with ethoxide derived from dissociative adsorption of ethanol, and a high reaction temperature such as 673 K is necessary to overcome the strong interaction between ethoxide and the MgO surface. It should be noted that the number of reactive intermediates involved in the production of butanol on MgO was not the same as the CO_2 adsorption capacity of MgO as measured by microcalorimetry.[66] This disparity highlights the problem of counting base sites with CO_2 at ambient temperature and attempting to relate the resulting adsorption site density to a catalytically relevant active site density. Nevertheless, the adsorption of a probe molecule such as CO_2 is very common in the characterization of metal oxide catalysts.

The coupling of methanol to higher alcohols can be hard to compare to the self-coupling of ethanol or propanol because rates of dehydrogenation are for both methanal and higher aldehyde production, and because methanal cannot form an enolate, the aldolization rate dependence on the concentrations of the two aldehydes is unclear. Some results not included in Table 1 involve the coupling of methanol and ethanol[68] as well as the coupling of methanol and C_2−C_5 primary alcohols.[69] Nevertheless, it is expected the general trends observed in Table 1 will hold for methanol and higher alcohol coupling rates over MgO. Other published works are excluded from the table because of a lack of necessary characterization information for the MgO used in the studies, such as specific surface area.

Many different promoters have been added to MgO to enhance its activity and selectivity to butan-1-ol. One common promoter is an alkali metal, such as lithium,[35] sodium,[35,68] potassium,[35] and cesium.[35,68] The addition of alkali metal salts, which likely imparted additional basicity to the catalyst, increased the selectivity to the dehydrogenation product, but not to the coupled product.[35,68] Unfortunately, there was no discussion in those papers of how the surface area might change after the addition of alkali metal promoters, so a direct comparison of areal rates on the materials is not possible. The influence of alkaline earth metals on the reactivity of MgO was also studied by Ndou et al.[46] and Ueda et al.;[68] however, no increase in the selectivity to the saturated, coupled alcohol products was observed over these materials.

3.2. Acid−Base Bifunctional Metal Oxides. Another approach to increase the activity of MgO for the coupling of alcohols is to increase the quantity of appropriate strength acid−base pairs. One method to increase these acid−base pairs is by incorporating Al, a stronger Lewis acid than Mg, into MgO. Preparation of Mg/Al mixed oxides is often accomplished by first synthesizing hydrotalcite layered materials (magnesium aluminum hydroxycarbonate), in which the brucite-like structure of $Mg(OH)_2$ is partially substituted with Al. Thermal decomposition of hydrotalcite gives well mixed oxides of Mg and Al. Mixed oxides prepared from hydrotalcites have been evaluated in a variety of reactions, including aldol condensation. In the aldol self-condensation of propanone and in aldol condensation of 3,7-dimethylocta-2,6-dienal with propanone and butan-2-one, the presence of Al with MgO promoted the rate compared with pure MgO.[39,70] The higher rate is thought to be the result of an increase in the quantity of appropriate acid−base pairs. In particular, the stronger Lewis acid Al may help by stabilizing the adsorbed intermediate.

In Table 3, rates associated with reactions in ethanol coupling over Mg/Al mixed oxides are presented. The catalyst entries are presented in the order of decreasing Mg content. As Al content in the mixed oxides increased, the rate of dehydration also increased, presumably the consequence of the new acid sites associated with Al. When a pure alumina catalyst or a mixed oxide rich in aluminum was used, the vast majority of the product was the dehydrated reactant, or ethene, because of the high density of strong acid sites.[71,72] Mixed oxides with high concentrations of Al revealed a product distribution that included buta-1,3-diene. For example, a Mg/Al mixed oxide (Mg/Al = 3) at a conversion of 50% had a 12% selectivity to buta-1,3-diene.[54] Direct comparison of the first two entries in Tables 1 and 3 reveals that a Mg/Al mixed oxide had a higher dehydrogenation rate. The observed increase in

dx.doi.org/10.1021/cs400292f | ACS Catal. 2013, 3, 1588−1600

the coupling rate over the mixed oxide is likely due to an increase in the gas phase aldehyde concentration and an increase in the aldol condensation rate over the bifunctional mixed oxide.

The acid and base properties of some of the Mg/Al mixed oxides presented in Table 3 have been evaluated with ammonia and carbon dioxide stepwise temperature-programmed desorption by Di Cosimo et al.,[31] and the results are summarized in Table 4. It should be noted that the acid−base site densities were evaluated by total uptake of the probe molecules at room temperature.[31] As the Al content in the mixed oxides increased, the ammonia uptake also increased. Comparing the rates of dehydration of ethanol and the uptake of ammonia for Mg/Al 8.1 (0.017 nmol m^{-2} s^{-1} and 0.81 μmol m^{-2}) and the Mg/Al 1.1 (0.16 nmol m^{-2} s^{-1} and 1.57 μmol m^{-2}), there appears to be some relationship between the two. Further characterization of the acid character of these samples would shed light on the relationship between the Al content and the dehydration rate. Likewise, the CO_2 adsorption capacity was correlated to the rate of dehydrogenation.[31] Comparing the rate of dehydrogenation of ethanol to the uptake of carbon dioxide for Mg/Al 8.1 (1.3 nmol m^{-2} s^{-1} compared with 1.17 μmol m^{-2}) and the Mg/Al 1.1 (0.081 nmol m^{-2} s^{-1} compared with 0.83 μmol m^{-2}), a relationship between carbon dioxide adsorption and ethanol dehydrogenation rates is seen.

Table 4. Acid and Base Properties of MgO, Al_2O_3, and Mg/Al Mixed Oxides Presented in Di Cosimo et al.[31,a]

material	total evolved CO_2 (μmol m^{-2})	total evolved NH_3 (μmol m^{-2})
MgO	1.63	0.48
Mg/Al 8.1	1.17	0.81
Mg/Al 4.6	0.46	0.84
Mg/Al 1.1	0.83	1.57
Mg/Al 0.5	0.73	1.39
Al_2O_3	0.34	1.34

[a]Adsorption of gas phase probe was completed at room temperature.

Mixed oxides of MgO and ZrO_2 are another well-known family of acid−base bifunctional materials that we have recently employed as catalysts for ethanol coupling.[67] Table 5 presents the rates of ethanol dehydration, dehydrogenation, and coupling along with the initial heat of adsorption and capacity for ammonia and carbon dioxide as measured by adsorption microcalorimetry. Pure zirconia had the highest density of acid sites titrated by ammonia adsorption and was quite active for ethanol dehydration to ethene. Thus, the presence of ZrO_2 at the surface of the mixed oxide was detrimental to the performance of MgO. As one might expect, the synthesis method used to prepare the mixed oxides of Mg and Zr significantly impacted the selectivity to the undesired product ethene. The rising pH precipitation method, which involved dissolving the metal precursors in water and then precipitating the mixed oxide/hydroxide with aqueous NaOH, produced a final material with fewer acid sites and, therefore, a lower observed rate of ethanol dehydration. In contrast, a material precipitated at a "controlled pH" at which the aqueous metal precursors were added to a vessel held at a constant pH had a higher number of acid sites and therefore a higher rate of ethanol dehydration compared with the sample prepared by the rising pH precipitation method. The microstructure of the final coprecipitated material was manipulated by exploiting the different pH at which MgO and ZrO_2 precipitate individually.[67]

Zirconia is generally regarded as an amphoteric oxide surface exposing both acid and base sites, which is confirmed by the uptake of ammonia and carbon dioxide reported in Table 5. As mentioned above, the acidity of zirconia effectively catalyzes the dehydration of ethanol preferentially over the dehydrogenation reaction, which is required for the coupling reaction. In an attempt to modify the acid−base character of zirconia, we added small amounts of Na onto ZrO_2 and tested the promoted catalysts in the coupling of ethanol.[73] The influence of Na loading on the adsorption capacity and the initial heat of adsorption of ammonia and carbon dioxide evaluated by microcalorimetry is presented in Table 6. As anticipated, the adsorption capacity and adsorption strength of CO_2 increased with Na loading presumably because Na created new basic sites on the zirconia surface. In contrast, the presence of Na neutralized a fraction of the surface acid sites titrated by adsorbed ammonia. The rate of ethanol conversion at 673 K and the selectivites to the products reported at similar conversion over the same three catalysts are shown in Table 7. Addition of Na to zirconia effectively reduced the unproductive dehydration of ethanol to ethene by neutralizing

Table 6. Summary of Results from Carbon Dioxide and Ammonia Adsorption Microcalorimetry on Zirconia with Various Amounts of Na[73]

	CO_2 adsorption		NH_3 adsorption	
Na content (wt %)	uptake[a] (μmol m^{-2})	initial $-\Delta H$ (kJ mol^{-1})	uptake[a] (μmol m^{-2})	initial $-\Delta H$ (kJ mol^{-1})
0	1.4	104	3.3	126
0.1	1.8	137	3.3	98
1	3.6	158	1.7	91

[a]Uptake calculated by extrapolating the saturation conditions to zero pressure.

Table 5. Summary of Results from Adsorption Microcalorimetry of Ammonia and Carbon Dioxide and Rates of Ethanol Conversion on Mg and Zr Containing Oxides at 673 K[67]

		NH_3 adsorption				CO_2 adsorption	
catalyst	ethene formation rate (nmol m^{-2} s^{-1})	coverage (μmol m^{-2})	initial $-\Delta H$ (kJ mol^{-1})	ethanal formation rate (nmol m^{-2} s^{-1})	butan-1-ol formation rate (nmol m^{-2} s^{-1})	coverage (μmol m^{-2})	initial $-\Delta H$ (kJ mol^{-1})
MgO[a]	6.6	0.70	120	15	1.1	0.83	162
Mg/Zr 11:1b[b]	12	0.73	84	15	0.8	0.74	185
Mg/Zr 11:1[a]	19	0.73	141	19		0.91	187
ZrO_2[a]	180	3.5	170	10		0.81	123

[a]Sample prepared by controlled pH precipitation. [b]Sample prepared by rising pH precipitation.

dx.doi.org/10.1021/cs400292f | ACS Catal. 2013, 3, 1588−1600

Table 7. Selectivity of the Products during Ethanol Coupling Reactions at 673 K and at Similar Conversions for Sodium-Doped Zirconia[73]

			selectivity (C%)[d]			
nominal Na (wt %)	ethanol conversion rate (nmol m^{-2} s^{-1})	conversion (%)	ethene	ethanal	but-2-enal	butan-1-ol
0[a]	200	9.4	44	54	0.0	2.2
0.1[b]	160	9.6	32	63	2.5	2.7
1[c]	40	7.7	17	71	0.0	12

[a]Reactant flow rate: 2.1 $\mu mol_{ethanol}$ m^{-2} s^{-1}. [b]Reactant flow rate: 1.7 $\mu mol_{ethanol}$ m^{-2} s^{-1}. [c]Reactant flow rate: 0.52 $\mu mol_{ethanol}$ m^{-2} s^{-1}. [d]Carbon-based selectivity.

a significant fraction of the surface acid sites responsible for the reaction, consistent with results from ammonia adsorption. Thus, the selectivity to aldehyde and coupling products increased at higher Na loading, primarily because of the decrease in dehydration. A comparison of different rates revealed addition information about the system. For example, the rate of acetone condensation was enhanced by addition of Na, as expected from the presence of new base sites. However, the rate of ethanol coupling was not increased over the Na-loaded materials, even at similar concentrations of ethanal in the gas phase. The kinetics of the reaction suggest that the coupling of ethanol is dominated by a large surface coverage of ethoxide,[73] analogous to that observed by isotopic transient analysis of ethanol coupling over MgO as discussed earlier.[66] The coverage of ethanol at reaction conditions evidently plays a major role in the rate of production of butan-1-ol from ethanol, and trends based on base site strength and density can be misleading, since more strongly bound ethoxide may decrease the available sites for the coupling step.

3.3. Hydroxyapatite. Another example of an acid−base bifunctional material used in the coupling of alcohols is hydroxyapatite, $Ca_5(PO_4)_3OH$. Table 8 summarizes the reaction rates for ethanol conversion over hydroxyapatites compared with calcium oxide and tricalcium phosphate. The hydroxyapatite materials were more effective at coupling and dehydrogenation compared to calcium oxide. Although tricalcium phosphate (β-TCP) showed a higher rate of alcohol coupling compared with the hydroxyapatite, it had a much higher selectivity to the undesired olefin, which may be a consequence of operating at much higher temperatures. In addition, the selectivity to the dehydrogenation and coupling products increased as the Ca content of the samples increased. Although a direct comparison of the rates in Table 8 is complicated by the wide variety of different temperatures used, a complete summary is provided to allow comparison with other materials, such as the Mg/Al mixed oxides in Table 3.

Similar to the Mg/Al mixed oxides, the rates of dehydration and dehydrogenation over hydroxyapatites are impacted by the composition of the catalyst. As the calcium content of the catalysts increased from Ca-deficient materials (Ca/P = 1.59)

Table 8. Rates for Ethanol Dehydration, Dehydrogenation, and Self-Coupling over Hydroxyapatite, Hydroxyapatite with Subsituted Strontium and Orthovanadate, Calcium Oxide, and Tricalcium Phosphate

material	surface area (m^2 g^{-1})	temp(K)	conversion	ethanal concn (μmol L^{-1})	dehydrogenation rate (nmol m^{-2} s^{-1})	dehydration rate (nmol m^{-2} s^{-1})	coupling rate others (nmol m^{-2} s^{-1})	coupling rate saturated alcohol (nmol m^{-2} s^{-1})	ref
β-TCP	1.2	678	10	62	77	58	24	54	55
β-TCP	1.2	709	20	105	137	168	40	94	55
Ca/P 1.59	27.5	644	10	15	2.0	35	0	0	55
Ca/P 1.59	27.5	660	20	21	2.9	73	0	0	55
Ca/P 1.62	35.7	593	10	24	2.0	2.2	2.7	7.2	55
Ca/P 1.62	35.7	623	20	31	2.8	9.7	3.0	11	55
Ca/P 1.65	40.3	548	10	11	0.58	0.18	1.8	6.7	55
Ca/P 1.65	40.3	569	20	12	0.68	0.40	3.7	14	55
Ca/P 1.67	37.8	545	10	8.1	0.42	0.10	1.7	6.7	55
Ca/P 1.67	37.8	571	20	12	0.65	0.23	3.5	13	55
Ca/P 1.69	58.7	573	7.1	0.24	0.007	0.00	0.88	2.6	32
CaO	6.4	670	10	79	23	47	0.26	1.1	55
CaO	6.4	694	20	108	32	97	0.94	2.0	55
Sr/P 1.57[a]	89	573	1.2	7.3	0.08	0.12	0.01	0.006	74
Sr/P 1.71	40.0	573	4.4	0.4	0.009	0	0.34	1.9	74
Sr/P 1.68	26.2	573	7.6	0.78	0.019	0.00	0.58	2.5	32
Ca/V 1.73	26	573	6.6	6.3	0.55	906	0.52	2.1	32
Sr/V 1.69	15.3	573	5.8	56	0.40	75	0.057	0.057	32

[a]Diethyl ether was a major component of the product stream.[74]

dx.doi.org/10.1021/cs400292f | ACS Catal. 2013, 3, 1588−1600

to stoichiometric materials (Ca/P = 1.67), the rate of dehydration decreased. The densities of acid and base sites, measured by ammonia and carbon dioxide adsorption at 523 K, respectively, are reproduced from Tsuchida et al.[55] in Table 9.

Table 9. Acid and Base Properties of Tricalcium Phosphate, Hydroxyapatite with Different Ca/P Ratios, and Calcium Oxide As Presented in Tsuchida et al.[55,a]

material	CO_2 adsorption site density (μmol m^{-2})	NH_3 adsorption site density (μmol m^{-2})
β-TCP	0.6	0.008
Ca/P 1.59	0.01	0.038
Ca/P 1.62	0.02	0.029
Ca/P 1.65	0.38	0.011
Ca/P 1.67	0.53	0.0006
CaO	0	0

[a]Adsorption of gas phase probe was completed at 523 K.

The decrease in dehydration rate with increasing Ca content of the samples correlated well with the observed decrease in acid site density and increase in base site density (Table 9). A direct comparison of the rates for samples with different Ca content is difficult because the reaction temperatures were not the same, but a relationship between dehydration rate and acid site density is apparent as well as a relationship between dehydrogenation rate and base site density.

Comparing the Mg/Al 8.1 mixed oxide catalyst (Table 3) and the Ca/P 1.67 hydroxyapatite catalyst (Table 8) at 573 and 571 K, respectively, the hydroxyapatite exhibited about a 50 times higher coupling rate, even with a lower gas phase ethanal concentration. In addition, hydroxyapatite prepared with strontium instead of calcium revealed a slightly higher rate of dehydrogenation than observed with calcium hydroxyapatite.[32] Because some of the Sr-substituted hydroxyapatites could have had significant amounts of residual Na, which can have a large impact on the acid and base properties of the surface as well as the reactivity of ethanol, those entries have not been included here.[74] Fortunately, two samples were precipitated with ammonia, thus allowing for a reasonable comparison with the other hydroxyapatite catalysts. The reactivity of a material with Sr/P 1.71 was similar to that of hydroxyapatite reported elsewhere, but a direct comparison is made difficult because of the large differences in conversion. Hydroxyapatite with a Sr/P ratio of 1.57 exhibited higher rates of dehydrogenation and productivities of acid-catalyzed reactions (i.e., production of diethyl ether and ethene) than one with a Sr/P ratio of 1.71.[74] Evidently, hydroxyapatites that are deficient in either Sr or Ca exhibit significant acidic character.[32,55,75]

Hydroxyapatites have been used as catalysts in a variety of other reactions of relevance to alcohol coupling. In particular, they have been used in the MPV hydrogen transfer from 2-butanol to 3-pentanone between 435 and 552 K[76] and for the dehydrogenation of alcohols.[76−78]

3.4. Basic Zeolites. Ethanol coupling has been performed over ion-exchanged and rubidium-impregnated zeolite X catalysts; reactivity results are summarized in Table 10. The rates are normalized by the grams of catalyst because the surface areas were not reported.[45] Although it is unclear how the surface area might be affected by the impregnation of Rb, zeolite 13X has an approximate surface area of 600−700 m^2 g^{-1}. The rates in Table 10 were determined at 693 K and indicate zeolites have some potential for the reaction, but direct comparisons to MgO, hydroxyapatite and the Mg/Al mixed oxides are not possible because surface area, ethanol concentrations, and conversions were not reported.

If the surface area of Rb−NaX were assumed to be 600 m^2 g^{-1}, then the rates for dehydrogenation and production of butanol are estimated to be 4.8 and 6.9 nmol m^{-2} s^{-1}, respectively. This calculated rate of coupling is similar to the reported rate of propan-1-ol coupling over MgO at 673 K[35] (8.2 nmol m^{-2} s^{-1}) and ethanol coupling over MgO at 658 K[55] (2.0 nmol m^{-2} s^{-1}).

Yang and Meng[45] reported decent selectivity to the coupled product at 693 K. It is important to note that zeolites without excess Rb were active for dehydrogenation but not for alcohol coupling. Evidently, the occluded Rb species was required for the aldol condensation step in the coupling sequence. The total rate of ethanol conversion (dehydrogenation rate + coupling rate × 2) for the Rb-promoted samples was reminiscent of the results reported by Hathaway and Davis[79] for dehydrogenation of propan-2-ol over Cs-impregnated CsNaX (cesium acetate-impregnated CsNaX) compared with purely ion-exchanged zeolite X (CsNaX). Hathaway and Davis[79] also studied other samples for the dehydrogenation of propan-2-ol and observed that CsAce/CsNaY had an activity similar to that of MgO, and both had higher activity than CsAce/CsNaX. Both Cs-impregnated X and Y zeolites were more active dehydrogenation catalysts than the ion-exchanged zeolites (CsNaY or CsNaX).

3.5. Dehydrogenation versus Dehydration. To help understand the effect of adding Lewis acid components on the catalysis of alcohol coupling, it is necessary to revisit the possible reaction mechanisms of the Guerbet reaction. In the next two sections, some of the speculated routes for conversion of intermediate species on metal oxide surfaces are presented. The intention of these sections is not to declare which mechanistic speculations are valid or invalid, but is to describe how the subtle interplay between reactive intermediates on exposed Lewis acid sites (metal cations) and surface base sites

Table 10. Rates for Ethanol Dehydration, Dehydrogenation, and Self-Coupling Zeolites Published by Yang and Meng[45]

material	temp (K)	dehydrogenation rate (μmol $g_{catalyst}^{-1}$ s^{-1})	coupling rate others (μmol $g_{catalyst}^{-1}$ s^{-1})	coupling rate saturated alcohol (μmol $g_{catalyst}^{-1}$ s^{-1})
LiX	693	3.5	0	0
NaX	693	2.9	0	0
KX	693	2.4	0	0
Rb−LiX	693	2.4	0.75	4.3
Rb−NaX	693	2.9	1.1	4.0
Rb−KX	693	3.4	0.35	1.7

dx.doi.org/10.1021/cs400292f | ACS Catal. 2013, 3, 1588−1600

Scheme 9. Proposed Mechanisms of Alcohol Dehydration and Dehydrogenation over MgO[a]

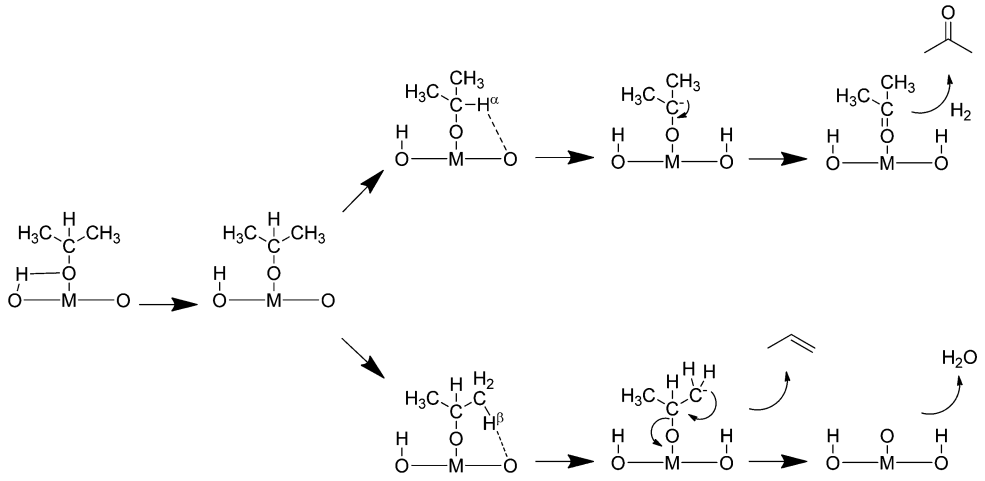

[a]This figure is adapted from Diez et al.[85]

(O or OH surface species) might affect the ethanol coupling reaction.

The first transformation in the Geurbet reaction converts the alcohol to either an aldehyde (dehydrogenation) or an olefin side product (dehydration). Dehydrogenation has been proposed to proceed via two different elementary steps on mixed oxides. The first surface intermediate is an adsorbed alkoxide, coordinated to a Lewis acid through the oxygen atom of the alkoxide with the dissociated hydrogen residing on a neighboring surface oxygen atom. The abstraction of hydrogen from an alcohol has been shown to occur over low-coordinated Mg and O atoms on MgO, which are present at corners, edges, and defects.[80−82] The adsorbed alkoxide of ethanol and methanol has been observed on MgO by DRIFTS even at room temperature.[83,84] Since the alkoxide is formed easily over basic oxides, it is likely the next step that is limiting the formation of the aldehyde on MgO.

The subsequent step involves the activation of the C−H bond of the adsorbed alkoxide and has been proposed to proceed by two slightly different reactions. The two proposed reactions include a second hydrogen atom removal with a basic oxygen shown in Scheme 9 or the combination of the adsorbed hydrogen from the alcohol group with the second hydrogen on the carbon atom associated with the C−O bond shown in Scheme 10. In Scheme 9, each hydrogen involved in the reaction is transferred via interaction with the surface oxide anion, whereas in Scheme 10, the hydrogen recombination reaction involves direct hydrogen transfer to a surface hydroxyl group.

Scheme 10. Proposed Mechanisms of Dehydration and Dehydrogenation[a]

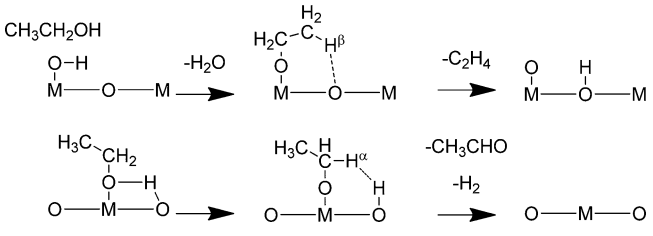

[a]Adapted from Shinohara et al.[86]

Although the difference between Schemes 9 and 10 is small, the location of the transferred hydrogen could impact the subsequent hydrogenation steps in the alcohol coupling mechanism. Hydrogen is needed to hydrogenate the products from the aldol condensation and can be derived from three sources: adsorbed hydrogen atoms produced from ethanol dehydrogenation, gas phase dihydrogen produced from ethanol dehydrogenation, or direct H transfer from the ethanol as in the MPV reaction. Interestingly, Gines and Iglesia included gas phase dideuterium in the reactant mixture during alcohol coupling and observed little incorporation of deuterium into the saturated coupled alcohol product formed over a mixed oxide ($K-Mg_5CeO_x$).[29] Therefore, gas phase dihydrogen is not the likely source of hydrogen for subsequent hydrogenation steps over mixed oxide samples. The MPV reaction and reactions involving surface hydrogen are more likely to play an important role in the hydrogenation steps over basic oxides or phosphates. Indeed, a surface alkoxide has been proposed to be the key intermediate in the MPV reaction over metal oxides. For more information on MPV reactions and the catalysts that perform them, please see a review by Ruiz and Jiménez-Sanchidrián.[87] As discussed previously, the nature of the acid and base pairs on the catalytic surface is likely to play an important role in the dehydrogenation reaction.

Dehydration reactions on the basic oxides can also occur via two separate pathways. The first proposed mechanism has been called a base-catalyzed dehydration, or more succinctly, an E_{1cB} mechanism. This proposed dehydration mechanism is shown in the bottom half of Scheme 9.[85] The key step is the removal of the β-hydrogen from the adsorbed alkoxide. The intermediate would have to be stabilized with an interaction between the oxygen and the surface Lewis acid ($Mg^{\delta+}$ in MgO). The carbanion intermediate formed with this proposed dehydration mechanism would be quite similar to the carbanion intermediate formed as an intermediate in the base-catalyzed aldolization, the only difference involving an additional hydrogen on the C−O carbon in the case of dehydration.

The second proposed dehydration intermediate, by an E_1-type mechanism, is shown in the top half of Scheme 10.[86] This reaction would also proceed through a stable alkoxide intermediate, which has been confirmed spectroscopically during Brønsted acid-catalyzed dehydration over zeolites.[88] Obviously, the mechanism for dehydration over MgO or other

dx.doi.org/10.1021/cs400292f | ACS Catal. 2013, 3, 1588−1600

oxides would depend on the reaction temperature and catalyst pretreatment conditions. Although MgO is typically thought to dehydrate alcohols through the E_{1cb} mechanism,[89] other basic oxides and mixed metal oxides may have different kinds of Lewis and Brønsted sites available for catalysis.

For both dehydrogenation and dehydration, the nature of the acid−base pair on the surface dictates the selectivity of the products formed. For a more thorough discussion on acid and base pair chemistry in metal oxides, see Iglesia et al.[90]

3.6. Aldolization. The aldolization of molecules possessing a carbonyl is a well known reaction in organic chemistry. On a solid catalyst, the adsorption of the carbonyl group is likely to occur on an electron-accepting or Lewis acid site. This site stabilizes the molecule and allows for the base-catalyzed removal of a hydrogen atom from the α-carbon. This hydrogen removal step forms a surface enolate in which the carbanion can then attack a nearby adsorbed aldehyde or ketone.[62] The resulting surface aldol product can then desorb, dehydrate and desorb; crack to produce products such as 2-propanone from the aldol product of ethanal; perform another aldolization; or continue reacting to produce a completely hydrogenated product, as in the Guerbet reaction.

Aldolization has also been shown to be promoted by bifunctional acid−base materials. Examples of bifunctional solids include Y^{3+} added to MgO,[91] Mg/Al mixed oxides,[39,41,70,92] amorphous aluminophosphate,[40] Cs/ZrO_2,[93] and Mg/Zr mixed oxides.[94,95] The promotion of the reaction on bifunctional catalysts is thought in part to be the result of the stabilization of a surface intermediate through a Lewis acid interaction. This interaction also allows large networks of aldolization products to form at elevated temperatures, since a strong interaction between the oxygenated intermediates and the Lewis acid sites prevents desorption, especially when multiple functional groups exist in one molecule.[91]

There have been many theoretical and experimental studies on aldol condensation over MgO. In particular, 2-propanone condensation has received significant attention. The formation of an enolate on MgO has been shown to occur at room temperature,[96] and the rate of 2-propanone condensation can be calculated from the results of Zhang et al.[43] at 273 K to be 54 nmol m^{-2} s^{-1} in liquid acetone (13.8 M) based on density[97] at 273 K. This aldol condensation rate over MgO at 273 K is higher than the reported alcohol coupling rates over MgO at temperatures as high as 773 K, as summarized in Table 1. Because aldol condensation readily occurs at low temperature, it is likely the dehydrogenation step limits the alcohol coupling reaction over basic metal oxides and phosphates.

4. CATALYSTS WITH TRANSITION METAL COMPONENTS

Catalysts composed of a basic support and a transition metal have an advantage over basic metal oxides for the Guerbet reaction. Use of a metal promoter enhances the ability, in some instances, to operate at lower temperatures because the dehydrogenation of the alcohols occurs much more readily over metals than over metal oxides such as MgO; however, if the reaction temperature is too high, decomposition of the reactant can cause a decrease in selectivity to the desired saturated alcohol.

Carlini and co-workers[27,98] have studied various metals on the same Mg/Al mixed oxide support for the coupling of methanol with propan-1-ol in a batch reactor at 473−493 K and 3 MPa. The metals (Pd, Ni, Rh, and Cu) were either supported on the basic mixed metal oxide or supported on carbon and added as a physical mixture.[98] The researchers observed that the best physical mixture was copper chromite and Mg/Al mixed oxide.[98] Copper chromite and the Mg/Al mixed oxide were better than physical mixtures of a metal (Pd, Ni, or Rh) on carbon with the Mg/Al mixed oxide. It was also observed that the metals Pd, Ni, and Rh showed no improvement when supported on the Mg/Al oxide compared with the physical mixture of the metal on carbon and the Mg/Al mixed oxide. However, copper supported on the Mg/Al oxide showed an increased rate and selectivity to the coupled product compared with the other physical mixtures and supported metals on Mg/Al mixed oxide catalysts.[98]

A recent publication by Marcu et al. presented ethanol reactivity over Mg/Al oxide supported metals, including Pd, Ag, Mn, Fe, Cu, Sm, and Yb.[99] Supported Pd and Cu showed the highest rates of butan-1-ol production of 14.5 nmol m^{-2} s^{-1} and 8.8 nmol m^{-2} s^{-1}, respectively. Those experiments were carried out in an autoclave reactor at 473 K and autogenic pressure. The intrinsic rates decreased with increasing reaction time, which was speculated to be due in part to the water produced by the coupling reaction altering the Mg/Al mixed oxide support. Water addition to the reactant mixture decreased the rates of butan-1-ol production, supporting the hypothesis that water has a detrimental effect on the catalyst. The study did not investigate possible leaching of active components into the ethanol medium at the elevated temperatures and pressures.[99]

A negative influence of water on the reaction of ethanol over Cu supported on Mg/Al oxides has also been observed.[100] Leon et al. explored the substitution of Al in Mg/Al mixed oxides with Fe.[101] Complete substitution of Fe into the Mg/Al materials caused a decrease in surface area from 142 m^2 g^{-1} for the Mg−Al material to 90 m^2 g^{-1} for the Mg−Fe material. More importantly, incorporation of Fe decreased the acid character of the materials and, hence, decreased the observed selectivity to ethene formed during ethanol conversion. A kinetic analysis suggested that ethanal is a key intermediate for the formation of C4 products, which is expected from the general mechanism of ethanol coupling reactions as discussed earlier. The role of Fe in the catalyst was less clear because, although it decreased the acid site density much more than the base site density as evaluated by adsorbed probe molecules, Fe might also enhance the conversion rate of ethanol to ethanal because it is a redox-active metal ion. The authors concluded that the Fe did not significantly influence the ethanol reaction to ethanal because the activation energy for the reaction was essentially unchanged. The role of Fe was therefore attributed mostly to a modification of the surface acid/base character of the oxide surface rather than the redox ability of the Fe.

Nagarajan and Kuloor[34] studied the addition of metal oxides to MgO on ethanol conversion. Their conditions were 573 and 623 K, 91.3 kPa, and a gas mixture of 50% H_2 and 50% ethanol in a flow reactor. The lower temperatures were necessary because at higher temperatures, especially over copper-containing materials, they noticed appreciable amounts of reactant decomposition. Among the metal oxides added to MgO (CuO, MnO, Cr_2O_3, ZnO, Al_2O_3, Fe_2O_3, UO_3, CeO_2, ThO_2, ZrO_2), promotional effects were noted after the addition of copper, iron, zinc, uranium, and manganese oxide to MgO.

Nagarajan and Kuloor[34] also studied three component systems consisting of MgO, a promoter metal oxide (iron, zinc, manganese or uranium), and copper, among which the highest yield of butan-1-ol observed was 36.4% over a catalyst

dx.doi.org/10.1021/cs400292f | ACS Catal. 2013, 3, 1588−1600

composition of 65:25:10 (MgO/CuO/MnO). The reactant feed was also varied in this work to include pure ethanal in one experiment and a 1:1 mixture of dihydrogen to ethanal in another experiment. In both cases, ethanal in the feed caused large amounts of coke to form on the catalyst. In the case without dihydrogen, but-2-enal was obtained at a yield of 10.2%, and in the case with dihydrogen, butan-1-ol was formed with a yield of 15.8%. As expected, dihydrogen in the reactant mixture together with copper in the catalyst facilitated hydrogenation of the ethanal condensation product.[34]

Another copper-containing material, potassium-promoted magnesia ceria mixed oxide (Mg_5CeO_x) with supported copper, has also been studied for alcohol coupling reactions by Gines and Iglesia.[29] Their experiments were carried out in a recirculating batch reactor at 573 K and 101.3 kPa. They documented the important role of Cu on activity and selectivity. When comparing the rates of ethanol dehydrogenation over catalysts with and without copper, large increases in dehydrogenation rates and coupling products were observed over copper-loaded samples. Initial rates were obtained for ethanol dehydrogenation over Mg_5CeO_x with 0.8 wt. % K and 0 wt % Cu (3.4 nmol m^{-2} s^{-1}) and a Mg_5CeO_x with 1.0 wt % K and 7 wt % Cu (240 nmol m^{-2} s^{-1}). Initial rates of formation of coupling products were also obtained for the same samples and were reported to be 0.16 and 0.76 nmol m^{-2} s^{-1} for the samples without copper and with copper, respectively. The increase in dehydrogenation rate for the sample with Cu probably caused the observed increase in the coupling rate through the increased concentration of the aldehyde in the gas phase.[29]

Gines and Iglesia[29] also observed that when copper was incorporated into the materials, the dehydrogenation and hydrogenation of alcohol and aldehyde, respectively, occur rapidly, which means that both alcohol and aldehyde will produce the coupled product. They also observed different incorporation rates of gas phase deuterium into the products when cofeeding dideuterium over materials, with and without copper. For the oxide catalyst without copper, very little deuterium was incorporated into the products, whereas for the copper-containing materials, deuterium was significantly incorporated in the products as well as in the reactants.[29] Both Gines and Iglesia[29] and Nagarajan and Kuloor[34] suggest that copper facilitates the dehydrogenation of the alcohol and promotes the hydrogenation reactions of the adsorbed coupling products.

The temperature and pressure used in the Gines and Iglesia[29] study were similar to the conditions used by Tsuchida et al.[55] for the most active hydroxyapatite catalyst, which allows for some comparisons. Although it is not possible to compare the coupling rates because they were reported at drastically different conversions, the dehydrogenation rate of the copper-containing material published by Gines and Iglesia[29] was about 370 times greater than that of hydroxyapatite with a Ca/P ratio of 1.67,[55] or 9 times greater if the coupling rates are also included in the calculation of a total dehydrogenation rate. The addition of Cu or other transition metal likely facilitates the dehydrogenation and provides greater amounts of surface H needed for the hydrogenation steps in the coupling reaction sequence. Although many of the metal-containing catalysts exhibit interesting rates and selectivities, additional studies that report the relevant properties of the metals, including dispersion and oxidation state of the metal component, are needed.

5. SUMMARY AND SUGGESTIONS

The Guerbet reaction or coupling of alcohols has seen a recent revival of interest, especially with the use of heterogeneous catalysts in the upgrading of short-chain alcohols. A preponderance of the literature indicates the reaction proceeds through an aldol-type intermediate, which requires the reactant alcohol(s) to first be dehydrogenated. Aldol-type coupling followed by dehydration and hydrogenation produces the Guerbet saturated alcohol product. Side reactions can completely deoxygenate the intermediate to form unsaturated hydrocarbons such as buta-1,3-diene from ethanol or cleave intermediates in the presence of water to form molecules such as acetone or 2-methylpropene from ethanol.

Although dehydrogenation of the reactant alcohol is a critical first step, it can be difficult to study at conditions similar to those used in the Guerbet reaction because of rapid conversion of intermediate aldehydes and ketones. However, primary alcohols that do not have an α-hydrogen, such as 2,2-dimethylpropan-1-ol, could be used as model reactants to shed light on this step. These dehydrogenation rates could be combined with model aldol condensations to provide an understanding of which steps are promoted over the different materials.

One interesting unresolved question in this area is how metal oxides and metal phosphates catalyze the hydrogenation of the aldol condensation products. Two likely paths include surface hydrogen that remains after alcohol dehydrogenation or from MPV hydrogen transfer from alcohol to the aldol condensation product. On copper, or on some other transition-metal-containing catalysts, there is rapid exchange with gas phase dihydrogen, so the hydrogenation and dehydrogenation mechanisms on metal-containing catalysts are likely different from those on metal oxides and phosphates.

The rates of alcohol dehydrogenation, coupling, and dehydration appear to be correlated to the acid−base properties of the materials as measured by adsorption of ammonia and carbon dioxide. Although direct measurements (i.e., adsorption microcalorimetry) of surface affinity and capacity for acid and base probe molecules provided more insights into the relationship between the acid and base properties and the reaction rates of reactant alcohol for the undesired (dehydration) and desired (dehydrogenation and coupling) products, they still did not correlate well with the observed coupling rates. In addition, instead of the standard acid site and base site probes (ammonia and carbon dioxide, respectively), different probe molecules may need to be used to interrogate the types of surface species believed to be active in this reaction. For example, carbonate (formed by CO_2 adsorption on basic metal oxides) is a very different structure from alkoxide (formed by alcohol adsorption on basic metal oxides). Whereas the overall adsorption capacities of acid and base sites of these materials are certainly part of the picture, additional information is still needed. The most active metal oxide or phosphate catalysts apparently have significant densities of weak acid and medium to strongly basic sites. What is not known is the proximity of the acid and base sites. New probes to study acid−base site pairs need to be developed.

One of the more promising techniques for the study of alcohol conversion reactions over basic oxides is isotopic transient analysis. This technique allows for the quantification of surface coverages of reactant and reactive intermediates as well as a turnover frequency that is independent of the number

of active sites estimated from the use of probe molecules used to count base (or acid) sites.

Although many materials have been explored for the Guerbet reaction, some of the most promising materials include copper-containing mixed oxides ($K-CuMg_5CeO_x$) and hydroxyapatite with a stoichiometric ratio of calcium to phosphate. Further investigation of acid−base properties of materials as well as their activity in the individual reaction steps that comprise the overall Guerbet reaction could provide information to further advance these and other materials for alcohol coupling.

AUTHOR INFORMATION

Corresponding Author

*E-mail: rjd4f@virginia.edu.

Notes

The authors declare no competing financial interest.

ACKNOWLEDGMENTS

This work was supported by the Chemical Sciences, Geosciences and Biosciences Division, Office of Basic Energy Sciences, Office of Science, U.S. Department of Energy, Grant no. DE-FG02-95ER14549.

REFERENCES

(1) Guerbet, M. *C.R. Acad. Sci. Paris* **1899**, 1002.
(2) O'Lenick, A. J. *J. Surfactants Deterg.* **2001**, *4*, 311−315.
(3) Fuchs, O. U.S. Patent 1,992,480 1931.
(4) Wibaut, J. P. U.S. Patent 1,910,582 1933.
(5) Fuchs, O. U.S. Patent 2,092,450 1937.
(6) Burgoyne, E. E. U.S. Patent 2,645,667 1951.
(7) Miller, R. E.; Bennett, G. E. U.S. Patent 2,762,847 1956.
(8) Miller, R. E. U.S. Patent 2,836,628 1958.
(9) Farrar, M. W.; Groves, W. U.S. Patent 2,971,033 1961.
(10) Pregaglia, G.; Gregorio, G. U.S. Patent 3,514,493 1970.
(11) Clark, R. U.S. Patent 3,972,952 1976.
(12) Abend, P. G.; Leenders, P. U.S. Patent 4,011,273 1977.
(13) Matsuda, M.; Horio, M. U.S. Patent 4,518,810 1985.
(14) Budge, J. R.; Compton, S. V. U.S. Patent 4,681,868 1986.
(15) Clark, A.; Condon, F. E. U.S. Patent 2,593,009 1952.
(16) Herzenberg, J.; Cevidalli, G.; Nenz, A. U.S. Patent 2,861,110 1958.
(17) Poe, R. L. U.S. Patent 3,328,470 1967.
(18) Yates, J. E. U.S. Patent 3,864,407 1975.
(19) Yates, J. E. U.S. Patent 3,979,466 1976.
(20) Carter, C. A. U.S. Patent 2,457,866 1949.
(21) Wilkinsburg, J. K.; Schulz, J. G. D. U.S. Patent 3,119,880 1964.
(22) Pregaglia, G.; Gregorio, G.; Conti, F. U.S. Patent 3,479,412 1969.
(23) Cull, N. L.; Mertzweiller, J. K. U.S. Patent 2,829,177 1958.
(24) Yang, K. W.; Jiang, X. Z.; Zhang, W. C. *Chin. Chem. Lett.* **2004**, *15*, 1497−1500.
(25) Carlini, C.; Macinai, A.; Marchionna, M.; Noviello, M.; Galletti, A. M. R.; Sbrana, G. *J. Mol. Catal. A: Chem.* **2003**, *206*, 409−418.
(26) Carlini, C.; Di Girolamo, M.; Macinai, A.; Marchionna, M.; Noviello, M.; Raspolli Galletti, A. M. R.; Sbrana, G. *J. Mol. Catal. A: Chem.* **2003**, *200*, 137−146.
(27) Carlini, C.; Flego, C.; Marchionna, M.; Noviello, M.; Galletti, A. M. R.; Sbrana, G.; Basile, F.; Vaccari, A. *J. Mol. Catal. A: Chem.* **2004**, *220*, 215−220.
(28) Carlini, C.; Girolamo, M. D.; Marchionna, M.; Noviello, M.; Galletti, A. M. R.; Sbrana, G. *J Mol. Catal. A: Chem.* **2002**, *184*, 273−280.
(29) Gines, M. J. L.; Iglesia, E. *J. Catal.* **1998**, *176*, 155−172.
(30) Kirk-Othmer Publishing *Kirk-Othmer Encyclopedia of Chemical Technology*, 5th ed.; Kroschwitz, J. I., Ed.; Wiley-Interscience: New York, 2004.
(31) Di Cosimo, J. I.; Apesteguía, C. R.; Ginés, M. J. L.; Iglesia, E. *J. Catal.* **2000**, *190*, 261−275.
(32) Ogo, S.; Onda, A.; Yanagisawa, K. *Appl. Catal., A* **2011**, *402*, 188−195.
(33) Nagarajan, V. *Indian J. Technol.* **1971**, *9*, 380−386.
(34) Nagarajan, V.; Kuloor, N. R. *Indian J. Technol.* **1966**, *4*, 46−54.
(35) Ndou, A. S.; Coville, N. J. *Appl. Catal., A* **2004**, *275*, 103−110.
(36) Veibel, S.; Nielsen, J. *Tetrahedron* **1967**, *23*, 1723−1733.
(37) Sanz, J. F.; Oviedo, J.; Márquez, A.; Odriozola, J. A.; Montes, M. *Angew. Chem., Int. Ed.* **1999**, *38*, 506−509.
(38) Davis, S. E.; Zope, B. N.; Davis, R. J. *Green Chem.* **2012**, *14*, 143−147.
(39) Abelló, S.; Medina, F.; Tichit, D.; Pérez-Ramírez, J.; Groen, J. C.; Sueiras, J. E.; Salagre, P.; Cesteros, Y. *Chem.—Eur. J.* **2005**, *11*, 728−39.
(40) Climent, M. J.; Corma, A.; Fornés, V.; Guil-Lopez, R.; Iborra, S. *Adv. Synth. Catal.* **2002**, *344*, 1090−1096.
(41) Di Cosimo, J. I.; Díez, V. K.; Apesteguía, C. R. *Appl. Catal., A* **1996**, *137*, 149−166.
(42) Zhang, G.; Hattori, H.; Tanabe, K. *Appl. Catal.* **1988**, *40*, 183−190.
(43) Zhang, G.; Hattori, H.; Tanabe, K. *Appl. Catal.* **1988**, *36*, 189−197.
(44) Oviedo, J.; Sanz, J. F. *Surf. Sci.* **1998**, *397*, 23−33.
(45) Yang, C.; Meng, Z. Y. *J. Catal.* **1993**, *142*, 37−44.
(46) Ndou, A. S.; Plint, N.; Coville, N. J. *Appl. Catal., A* **2003**, *251*, 337−345.
(47) Toussaint, W. J.; Lee Marsh, J. In *Synthetic Rubber*; Whitby, G. S., Ed.; Wiley: New York, 1954; pp 86−104.
(48) Kitayama, Y.; Satoh, M.; Kodama, T. *Catal. Lett.* **1996**, 95−97.
(49) Kitayama, Y.; Michishita, A. *J. Chem. Soc. Chem. Commun.* **1981**, 401−402.
(50) Gruver, V.; Sun, A.; Fripiat, J. *Catal. Lett.* **1995**, *34*, 359−364.
(51) Niiyama, H.; Morii, S.; Echigoya, E. *Bull. Chem. Soc. Jpn.* **1972**, *45*, 655−659.
(52) Kvisle, S.; Aguero, A.; Sneeden, R. P. A. *Appl. Catal.* **1988**, *43*, 117−131.
(53) Jones, M. D.; Keir, C. G.; Di Iulio, C.; Robertson, R. A. M.; Williams, C. V.; Apperley, D. C. *Catal. Sci. Technol.* **2011**, *1*, 267−272.
(54) Ordóñez, S.; Díaz, E.; León, M.; Faba, L. *Catal. Today* **2010**, *167*, 71−76.
(55) Tsuchida, T.; Kubo, J.; Yoshioka, T.; Sakuma, S.; Takeguchi, T.; Ueda, W. *J. Catal.* **2008**, *259*, 183−189.
(56) Sun, J.; Zhu, K.; Gao, F.; Wang, C.; Liu, J. *J. Am. Chem. Soc.* **2011**, *133*, 11096−11099.
(57) Nishiguchi, T.; Matsumoto, T.; Kanai, H.; Utani, K.; Matsumura, Y.; Shen, W.; Imamura, S. *Appl. Catal., A* **2005**, *279*, 273−277.
(58) Bussi, J.; Parodi, S.; Irigaray, B.; Kieffer, R. *Appl. Catal., A* **1998**, *172*, 117−129.
(59) Nakajima, T.; Nameta, H.; Mishima, S.; Matsuzaki, I.; Tanabe, K. *J. Mater. Chem.* **1994**, *4*, 853−858.
(60) Haga, F.; Nakajima, T.; Yamashita, K.; Mishima, S. *React. Kinet. Catal. Lett.* **1998**, *63*, 253−259.
(61) Nakajima, T.; Yamaguchi, T.; Tanabe, K. *J. Chem. Soc. Chem. Commun.* **1987**, 394.
(62) Lippert, S.; Baumann, W.; Thomke, K. *J. Mol. Catal.* **1991**, *69*, 199−214.
(63) Christensen, J. M.; Jensen, P. A.; Schiødt, N. C.; Jensen, A. D. *ChemCatChem* **2010**, *2*, 523−526.
(64) Nunan, J.; Bogdan, C.; Klier, K.; Smith, K. *J. Catal.* **1989**, *116*, 195−221.
(65) Xu, M.; Iglesia, E. *J. Catal.* **1999**, *131*, 125−131.
(66) Birky, T. W.; Kozlowski, J. T.; Davis, R. J. *J. Catal.* **2013**, *298*, 130−137.
(67) Kozlowski, J. T.; Behrens, M.; Schlögl, R.; Davis, R. J. *ChemCatChem* **2013**, DOI: 10.1002/cctc.201200833.
(68) Ueda, W.; Kuwabara, T.; Ohshida, T.; Morikawa, Y. *J. Chem. Soc., Chem. Commun.* **1990**, 1558−1559.

(69) Ueda, W.; Ohshida, T.; Kuwabara, T.; Morikawa, Y. *Catal. Lett.* **1992**, *12*, 97−104.
(70) Kustrowski, P.; Sulkowska, D.; Chmielarz, L.; Rafalskalasocha, A.; Dudek, B.; Dziembaj, R. *Microporous Mesoporous Mater.* **2005**, *78*, 11−22.
(71) Di Cosimo, J. I.; Díez, V. K.; Xu, M.; Iglesia, E.; Apesteguía, C. R. *J. Catal.* **1998**, *178*, 499−510.
(72) Carvalho, D. L.; De Avillez, R. R.; Rodrigues, M. T.; Borges, L. E. P.; Appel, L. G. *Appl. Catal., A* **2012**, *415*−*416*, 96−100.
(73) Kozlowski, J. T.; Davis, R. J. *J. Energy Chem.* **2013**, *22*, 58−64.
(74) Ogo, S.; Onda, A.; Iwasa, Y.; Hara, K.; Fukuoka, A.; Yanagisawa, K. *J. Catal.* **2012**, *296*, 24−30.
(75) Tsuchida, T.; Sakuma, S.; Takeguchi, T.; Ueda, W. *Ind. Eng. Chem.* **2006**, *45*, 8634−8642.
(76) Kibby, C.; Hall, W. *J. Catal.* **1973**, *31*, 65−73.
(77) Ogo, S.; Onda, A.; Yanagisawa, K. *Appl. Catal., A* **2008**, *348*, 129−134.
(78) Kibby, C.; Hall, W. *J. Catal.* **1973**, *29*, 144−159.
(79) Hathaway, P. E.; Davis, M. E. *J. Catal.* **1989**, *119*, 497−507.
(80) Branda, M. M.; Rodríguez, A. H.; Belelli, P. G.; Castellani, N. *J. Surf. Sci.* **2009**, *603*, 1093−1098.
(81) Petitjean, H.; Tarasov, K.; Delbecq, F.; Sautet, P.; Krafft, J. M.; Bazin, P.; Paganini, M. C.; Giamello, E.; Che, M.; Lauron-Pernot, H.; Costentin, G. *J. Phys. Chem. C* **2010**, *114*, 3008−3016.
(82) Branda, M. M.; Belelli, P. G.; Ferullo, R. M.; Castellani, N. J. *Catal. Today* **2003**, *85*, 153−165.
(83) Bailly, M.; Chizallet, C.; Costentin, G.; Krafft, J.; Lauron-Pernot, H.; Che, M. *J. Catal.* **2005**, *235*, 413−422.
(84) Kozlowski, J. T.; Aronson, M. T.; Davis, R. J. *Appl. Catal., B* **2010**, *96*, 508−515.
(85) Díez, V. K.; Apesteguía, C. R.; Di Cosimo, J. I. *Catal. Today* **2000**, *63*, 53−62.
(86) Shinohara, Y.; Satozono, H.; Nakajima, T.; Suzuki, S.; Mishima, S. *J. Chem. Software* **1998**, *4*, 41−50.
(87) Ruiz, J.; Jiménez-Sanchidrián, C. *Curr. Org. Chem.* **2007**, *11*, 1113−1125.
(88) Kondo, J. N.; Ito, K.; Yoda, E.; Wakabayashi, F.; Domen, K. *J. Phys. Chem. B* **2005**, *109*, 10969−10972.
(89) Aramendía, M. A.; Borau, V.; Jiménez, C.; Marinas, J. M.; Porras, A.; Urbano, F. J. *J. Catal.* **1996**, *161*, 829−838.
(90) Iglesia, E.; Barton, D. G.; Biscardi, J. A.; Gines, M. J. L.; Soled, S. L. *Catal. Today* **1997**, *38*, 339−360.
(91) Fouad, N. E.; Thomasson, P.; Knözinger, H. *Appl. Catal., A* **2000**, *196*, 125−133.
(92) Ma, C.; Liu, G.; Wang, Z.; Li, Y.; Zheng, J.; Zhang, W.; Jia, M. *React. Kinet. Catal. Lett.* **2009**, *98*, 149−156.
(93) Tai, J.; Davis, R. J. *Catal. Today* **2007**, *123*, 42−49.
(94) Sádaba, I.; Ojeda, M.; Mariscal, R.; Fierro, J. L. G.; Granados, M. L. *Appl. Catal., B* **2011**, *101*, 638−648.
(95) Barrett, C. J.; Chheda, J. N.; Huber, G. W.; Dumesic, J. A. *Appl. Catal., B* **2006**, *66*, 111−118.
(96) Lercher, J.; Noller, H.; Ritter, G. *J. Chem. Soc., Faraday Trans.* **1981**, *1*, 621−628.
(97) *Sasol Density Tables for Sasol Solvents and Sasol Acrylates Products in the range 0 to 40* °C; http://www.sasol.com/sasol_internet/downloads/Density_Solvents_1247742607357.pdf (accessed Nov 25, 2012).
(98) Carlini, C.; Marchionna, M.; Noviello, M.; Galletti, A. M. R.; Sbrana, G.; Basile, F.; Vaccari, A. *J. Mol. Catal. A: Chem.* **2005**, *232*, 13−20.
(99) Marcu, I.; Tanchoux, N.; Fajula, F.; Tichit, D. *Catal. Lett.* **2012**, *143*, 23−30.
(100) Marcu, I.; Tichit, D.; Fajula, F.; Tanchoux, N. *Catal. Today* **2009**, *147*, 231−238.
(101) León, M.; Díaz, E.; Vega, A.; Ordóñez, S.; Auroux, A. *Appl. Catal., B* **2011**, *102*, 590−599.